AIAA JOURNAL
Vol. 31, No. 4, April 1993

Experimental Investigation of Hypersonic Three-Dimensional Corner Flow

Hakan Papuccuoglu*
Istanbul Technical University, 80191 Istanbul, Turkey

The high heat transfer rates and flow pattern were investigated in the vicinity of a 90-deg axial corner at a Mach number of 6 and over a Reynolds number range from 7 to 22.5 × 10^6. The investigation was carried out for two different corner configurations, one that involves two 9-deg half-angle unswept intersecting wedges and the other one that consists of a 9-deg half-angle unswept wedge and a flat plate aligned with the freestream. In this study it was observed that, in some cases, there are three and even four peaks of aerodynamic heating in the corner region. To give a reasonable physical explanation for the results of the experiments, two different vortex systems have been developed qualitatively in the boundary layer. A sharp decrease of heating detected in the region very near the corner centerline is attributed to the mutual interaction of the surface boundary layers, as also indicated in the literature, and a pair of small vortices causing the flow to lift off the surface.

I. Introduction

IN the design of high-speed airplanes and space shuttles subject to hypersonic flow, it is necessary to understand the corner flow problem, which is locally very important. The corner flow problem can be considered as one including a strongly disturbed inviscid flowfield and, in turn, the interaction of this flowfield with the boundary layers on the surface of the wedges.[1] Corner flows exist in the parts of the aerodynamic vehicles such as the fuselage wing and fin body junctions, rectangular inlet diffusers, ducts of airbreathing engines, and intersections of several control surfaces. In these corners, extraordinarily complex structures of shock-wave/boundary-layer interactions occur that are accompanied by a considerable increase of both static pressure and heat transfer rate.

Early investigations[2,3] carried out for two intersecting flat plates at Mach numbers 4.95 and 8 revealed that there is a considerable increase of both static pressure and heat transfer rates in the corner region. The first experimental study, showing the flow structure in an axial corner of two intersecting compression wedges, was performed by Charwat and Redekopp.[4] Their study indicated that the wedge bow shocks are joined by a third corner shock, and the internal flow includes two slightly curved embedded shocks terminating at the wedge surfaces and two slip surfaces originating from the triple points and meeting one another at the corner centerline. Similar corner flow structure was shown for intersecting wedges by Watson and Weinstein[5] and for flat plates by Cresci et al.[6] in hypersonic streams. The investigation by Cooper and Hankey[7] for the single compression corner configuration showed two large vortices responsible for high local heating within the boundary layer. However, the position of the vortices gave rise to some doubts. Some experimental data that were obtained by West and Korkegi[8] and Korkegi[9] showed an improved picture of the inviscid wave structure in the corner region. In recent years, a comprehensive study that takes into account different corner structures (different leading-edge swept angles, corner angles, and wedge angles) has been done by Hummel.[10]

It is the purpose of this paper to investigate the physical mechanism responsible for high heat transfer rates and understand the flow pattern in the axial corner region.

Received Feb. 27, 1992; revision received July 6, 1992; accepted for publication July 31, 1992.

*Researcher, Faculty of Mechanical Engineering, Mechanics and Fluid Dynamics Department.

II. Experimental Apparatus and Conditions

The tests were run in the H-3 (Mach 6) wind tunnel of the von Kármán Institute. The wind tunnel is a blowdown facility equipped with a 15-cm exit diameter axisymmetric contoured nozzle and 12-cm uniform test core diameter. During the experiments the tunnel stagnation temperature is between 500 and 600 K, and it can remain constant for a running time of 1 min. The uncertainties due to the Mach number and unit Reynolds number variation are about ±2% and ±6%, respectively, for the H-3 Mach 6 wind-tunnel conditions. Freestream unit Reynolds numbers used in this paper are based on 1 m length in the y direction.

An inframetrics model 525 infrared scanning radiometer has been used for heat transfer measurements. It produces a video-compatible signal at a framing rate of 25 Hz with a 2:1 interlace. It has a field of view of 14 deg horizontal with a 4:1 electro-optical zoom and a maximum sensitivity of 0.2 K. The infrared camera was calibrated by heating the model surface with a 1 kW lamp to a given temperature and correlating the measured intensity during cooling of the model to the surface temperature as the latter is recorded by means of a surface thermocouple. Running time for infrared thermography method varies from 0.1 to 0.6 s, depending on the test conditions, and the initial time is determined as the time when minimum temperature increase on the model surface is detected by the infrared camera. To calculate the Stanton number, a semi-infinite slab principle was used. The average uncertainty in the Stanton number, which is calculated by means of the second power equation, is about ±9%. The standard deviation for this value is about 0.7%. Since running only one experiment provides a complete thermal map of the model surface and the real error is a fixed quantity for a certain experiment, the values of all of the points on the heat transfer distribution graphic will increase or decrease at the same ratio. Although the magnitudes of the heat transfer data may change, the peak aerodynamic heating regions cannot be eliminated due to the uncertainty.

To verify the heat transfer results obtained by the infrared thermography method, sublimation method experiments have been employed. The surface of the model, before coating with acenaphthene, was painted dark blue to obtain good contrast. Tunnel testing time for the sublimation method is approximately 2–4 s for the given test conditions. The surface flow pattern is determined by the oil flow and oil dot visualization method. For this purpose, talcum powder and titanium oxide were mixed with oil and a suitable mixture was obtained. The surface of the model was painted black and a good contrast

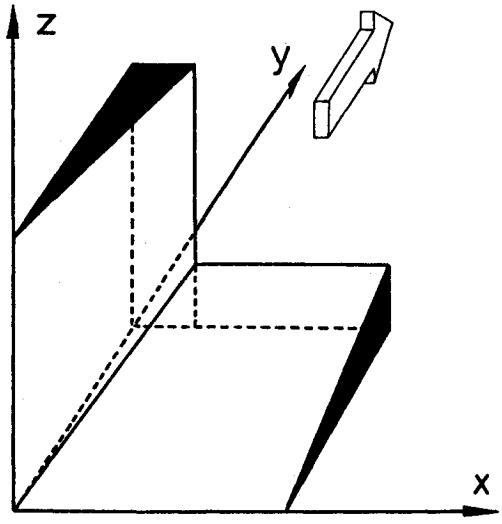

Fig. 1 Schematic of flow model.

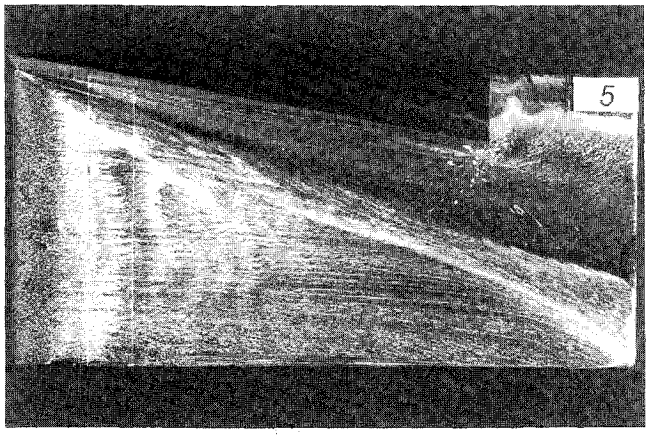

Fig. 2 Oil flow visualization (double comp. corner case $Re = 15.5 \times 10^6$).

was provided. Running times for oil dot and oil flow visualization methods are about 1 and 2 s, respectively.

The models were made of steel and covered with black Plexiglas. Since Plexiglas is a good insulator, during the heat transfer measurements the black Plexiglas does not absorb the heat quickly and the local heating regions are recognized easily. The width (in the x direction) and the length (in the y direction) of the model surface where the measurements were done are 10 and 21 cm, respectively. The z dimension of the model is 5 cm.

The interaction flow model shown in Fig. 1 represents a double compression corner (axial intersection of two wedges). The other model used for the experiments is a single compression corner (wedge on a flat plate). The coordinate system used in subsequent figures is illustrated in Fig. 1.

III. Presentation and Discussion of Results

A survey of literature and the results of the experiments confirmed that high heat transfer rates are located in the reattachment zones of a vortex system caused by the complex shock-wave/boundary-layer interactions.[1,3,7,9-11] The impingement of embedded shock on the boundary layer creates a pressure gradient and causes the boundary layer to separate. In three-dimensional separation, which is present in the axial corner flow case, the vortex is not trapped by the dividing streamline, and the flow entering the separated region is scavenged away. The scavenged flow is replenished by the oncoming part of the boundary layer that includes high-energy streamlines. Hence the reattaching streamline is a high-energy streamline. Since the heating in the reattachment region is proportional to the kinetic energy of the reattaching streamline, very high heating rates are observed in the three-dimensional reattachment region.[7]

A. Surface Flow Visualization

Examination of the surface flow pattern revealed that the flow is laminar, having a large interaction region at the beginning, and then transition is observed where a break on the outer separation line appears (Fig. 2). Beyond this break, the boundary layer becomes turbulent.[12] In the turbulent boundary-layer case, the interaction region is considerably narrower than that in the laminar boundary-layer case,[13] and the displacement effect of the boundary layer is comparatively small in the turbulent flow case, and so the whole shock system is slightly closer to the axial corner.[8]

In Fig. 3 a thick oil accumulation line indicates the location of the primary separation line that also shows the outer border of interaction.[1] The primary reattachment line corresponds to the dark region very near the secondary separation line.[14] It is very interesting to note that there is no break or curvature part on the secondary separation line. Therefore, as can be seen in Fig. 3, transition and turbulent flow regimes do not affect or change the shape of the secondary straight separation line. Between the primary and secondary separation lines, two oil accumulation lines are present that are not very clear (Fig. 3). As is seen in Fig. 4, a large outer disturbance zone is characterized by the primary separation line toward which skin friction lines or limiting streamlines converge asymptotically. The primary reattachment line, from which the skin friction lines diverge, is also apparent. If the three-dimensional corner flowfield is projected onto one of the wedges (e.g., x-y plane), a triangular region is obtained. The width (in the x direction) of this triangular region is zero at the corner apex. Therefore, it is evident that near the leading edge two-dimensional flow can be achieved for even small values of x. Examining the flowfield shown in Fig. 4 carefully, one can easily see that near the leading edge and far from the corner apex (for large x values) the straight limiting streamlines indicating the two-dimensional flowfield become curved only about 1.5 cm from the tip

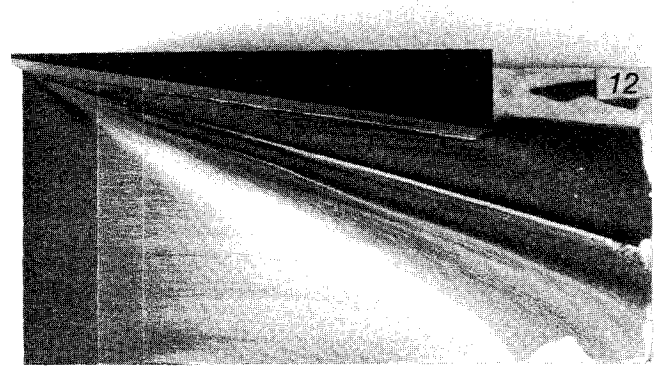

Fig. 3 Oil flow visualization (single comp. corner case $Re = 7 \times 10^6$).

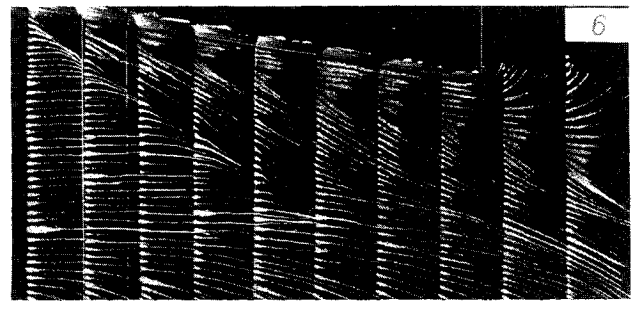

Fig. 4 Oil dot visualization (double comp. corner case $Re = 16.5 \times 10^6$).

of the wedge. Therefore, the tip effect is negligible in a distance more than 1.5 cm from the tip of the wedge for given test conditions. Since the curved limiting streamlines about 3 cm from the tip of the wedge cannot be caused by the tip effect, the brake on the outer separation line certainly indicates boundary-layer transition (Fig. 4). Surface oil flow patterns, in general, show a conical flow structure. However, the nonuniform displacement effect of the boundary layer changes the conical nature of the flowfield near the leading edge where hypersonic viscous interaction parameter $\bar{\chi}$ is larger than 4.[5] The occurrence of transition is another fact disturbing the conical nature of the viscous flowfield.

B. Surface Heat Transfer Distribution

Heat transfer distribution is obtained by employing infrared thermography and sublimation methods. In addition to having a complete thermal map of the model surface by means of sublimation and infrared thermography methods, in a specific rectangular region (4 × 5 cm), intensive heat transfer measurements are carried out using a teleoptic zoom lens to get high resolution. The heat transfer distributions in this specific region are presented by means of the line scans in the spanwise direction, which is 7.5 cm from the leading edge. Figures 5–8 show those spanwise heat transfer distributions for various

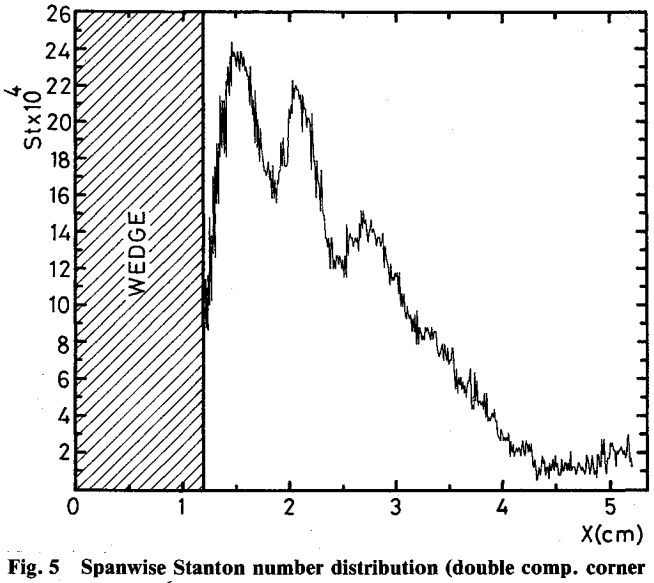

Fig. 5 Spanwise Stanton number distribution (double comp. corner case $Re = 15 \times 10^6$).

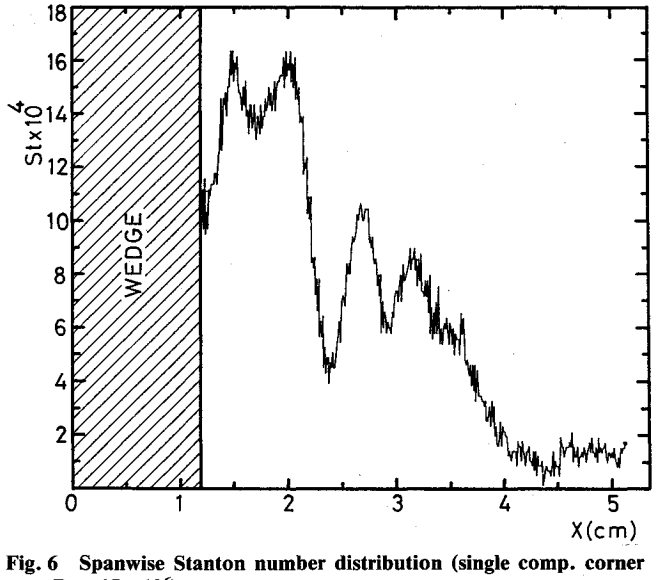

Fig. 6 Spanwise Stanton number distribution (single comp. corner case $Re = 15 \times 10^6$).

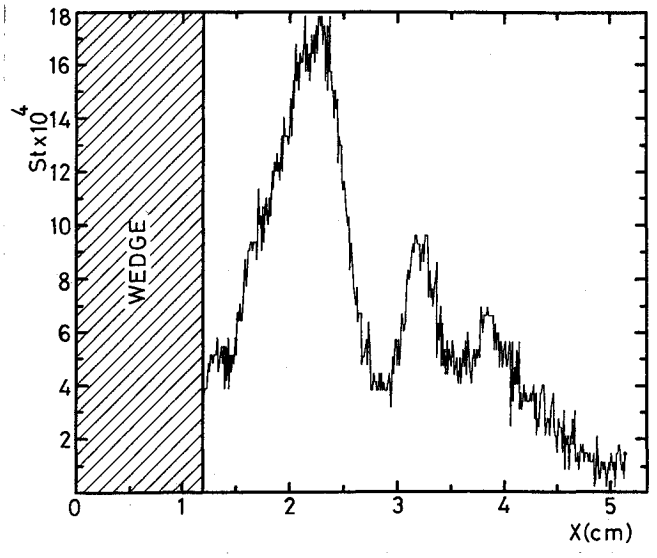

Fig. 7 Spanwise Stanton number distribution (single comp. corner case $Re = 7 \times 10^6$).

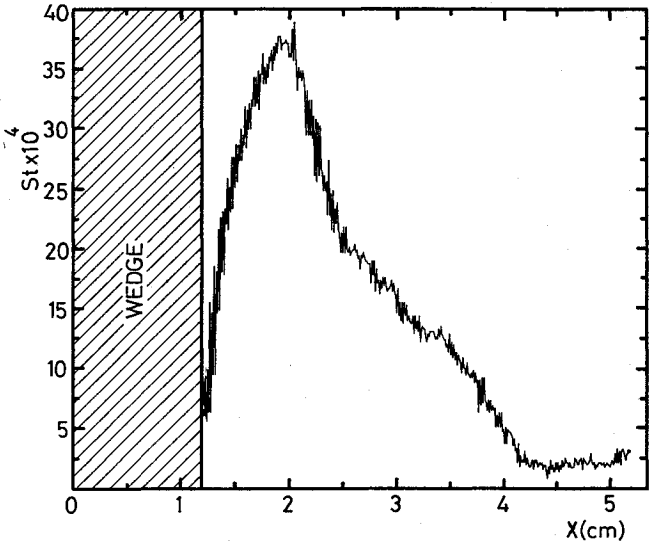

Fig. 8 Spanwise Stanton number distribution (double comp. corner case $Re = 21 \times 10^6$).

Reynolds numbers and single and double compression cases. For the single compression corner case, the data presented are for the surface aligned with freestream velocity. The dark regions seen in Figs. 9 and 10 indicate the regions of high shear stresses, and depending on these, the high heating rates are present. If a comparison is made between the thermography findings obtained by the sublimation method and infrared thermography results, similar heat transfer distributions are seen. Although it is quite impossible to make a quantitative comparison between the data obtained by those two methods about the severity of the high aerodynamic heating, the number of peaks and their positions are almost the same for both methods. For instance, there are four high skin friction regions exhibited in the form of dark lines in Fig. 9, and it is possible to match their positions with the peaks seen in Fig. 6. For example, in Fig. 9 the angle between the two dark lines, one of which is closest to and the other one furthest from the corner centerline, is about 12 deg. These lines show the approximate location of the primary and secondary reattachment lines, respectively. This angle can also be calculated from x and y coordinates of the leftmost and rightmost peaks in Fig. 6.

Fig. 9 Sublimation method (single comp. corner case $Re = 10 \times 10^6$).

Fig. 10 Sublimation method (double comp. corner case $Re = 8 \times 10^6$).

The heat transfer distributions show a marked dip or trough to values well below those for a two-dimensional wedge (in particular at the first separation line), followed by a sharp rise to multiple peaks. A decrease in aerodynamic heating is observed in the region very near the corner centerline. The maximum Stanton number, for a given unit Reynolds number, is almost constant with the Reynolds number based on the distance from the leading edge. This result has been verified before in Ref. 11. Except for the region where the hypersonic interaction parameter is high, the conical nature of the flowfield determined by infrared thermography is confirmed by the sublimation method as well. In Fig. 5, there are three peaks in the Stanton number, implying the existence of three vortices. For the same configuration (double compression corner case) at the large Reynolds number, however, only one peak occurs, implying only one vortex exists (Fig. 8). This drastic alteration is due to the principle that a turbulent boundary layer resists separation due to the turbulent mixing that fills out the velocity profile and thereby increases the average momentum of a turbulent boundary layer. At high unit Reynolds numbers, transition and then turbulent flow regimes occur closer to the leading edge. Since the location of the line scan indicating the heat transfer distribution is in the turbulent flow region (Fig. 8), there is only one separation and one reattachment line, indicating only one vortex. This result is in very good agreement with the findings of Ref. 11. For the same unit Reynolds number the aerodynamic heating in the double compression corner case is generally 1.5 times as high as in the single compression corner case.

C. Flow Structure

The combined evaluation of heat transfer distribution and oil flow visualization revealed that a vortex system responsible for high aerodynamic heating is present in the corner region. The study done by Korkegi[9] showed that the greater the shock strength or the wedge angle, the larger the extent of separation; for a large extent of the separation a secondary surface vortex arises inside the primary one. According to the data used in Korkegi's study,[9] depending on the shock strength, there were up to two peaks of heating associated with two reattachment points. In the present study, since the peak values of heating and the drops between the peaks are attributed to reattachment and separation zones, respectively, a vortex system consisting of four vortices (Fig. 11) and another one consisting of three vortices (Fig. 12) have been developed qualitatively. Note that the physical phenomenon, interaction of a skewed shock with the surface boundary layer, is the same for both cases[9] (single compression and double compression corner). Hence, no distinction is made between these two cases in evaluating the vortex systems seen in Figs. 11 and 12.

There is an embedded crossflow supersonic region in the viscous layer. This crossflow entering the corner region beneath the triple point eventually impinges on the surface of the wedge[15] and creates a high aerodynamic heating. Since the velocity and, depending on this, the kinetic energy of the streamlines originating from the outer parts of the boundary layer are high, the peak values of heating are located in the vicinity of the primary reattachment point R_1.[10] The inner vortices scavenge flow from the outer ones, and, in turn, the primary vortex between S_1 and R_1 scavenges flow from the oncoming boundary layer (Figs. 11 and 12).

The outer compression fan seen in Fig. 11 is a consequence of the supersonic crossflow and the displacement effect of the boundary layer,[5,8] and it is not a property of the inviscid flowfield as suggested by Chartwat and Redekopp.[4] Note that the outer compression fan does not have to be centered at the triple point. Since most of the authors prefer to show it as seen in the upper part of Fig. 11, this author follows the same manner.

Because of the nature of three-dimensional boundary layers, the surface flow pattern in the axial corner region could give a misleading impression that the entire flowfield is highly skewed from the streamwise direction (lower part of Fig. 12);

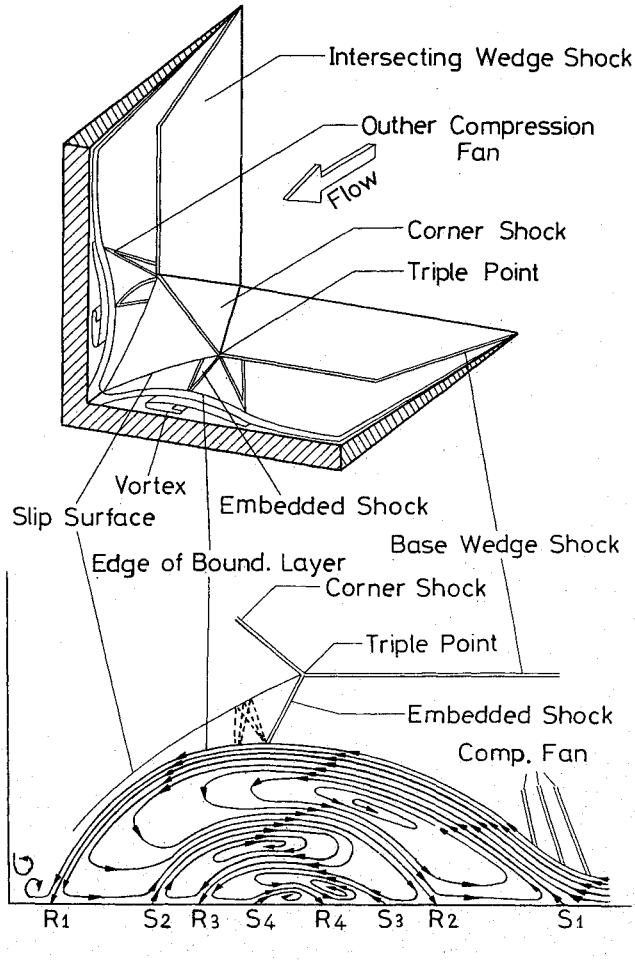

Fig. 11 Corner flow shock structure and vortex system for four vortices.

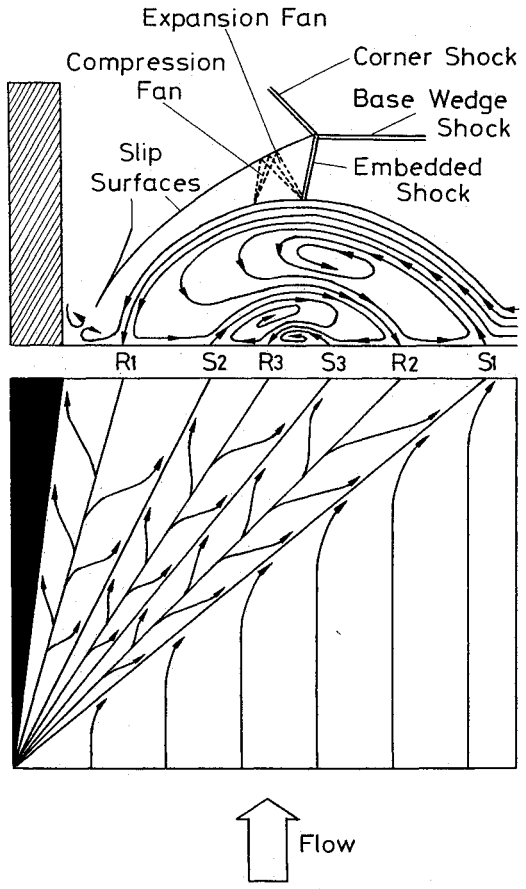

Fig. 12 Sketch of limiting streamlines and vortex system for three vortices.

however, most of the flow turning takes place over a thin region of fluid close to the wall.

The embedded shock impinging on the boundary layer is reflected from the boundary layer in the form of a fan of expansion waves. This expansion fan is reflected from the slip surfaces and impinges on the boundary layer as a compression fan.[10] The author suggests that the complex vortex system and multiple separation zones occurring in the axial corner region could be caused by the pressure gradients due to the embedded shock and this compression fan (Fig. 12).

Since on the wedge surfaces similar flowfields are present, the crossflow streamlines outside the separation bubble come from both sides of the corner and go toward the intersection line of the wedges. Because of the shape of the separation bubble and the thin boundary layer just around the axial corner, the streamlines coming toward one another form two small vortices. Although the high momentum of the crossflow streamlines create a compression in the corner region, the pair of small vortices cause the flow to lift off the small region very near the corner centerline (Fig. 11 and 12). The author suggests that the sharp decrease of heating in the very vicinity of the axial corner could be explained by the flow lifting off due to these small vortices. The author also believes that the mutual interaction of the surface boundary layers is another reason for the sharp decrease of heating as suggested in Refs. 3 and 11.

IV. Conclusion

Considering the heat transfer distribution and surface flow visualization analysis, three-dimensional vortex systems responsible for high aerodynamic heating were developed qualitatively in the corner region. Peak heating rates are located in the vicinity of the reattachment regions of the vortex systems. The vortex systems can include up to four vortices and separated zones depending on the test condition.

The author suggests that the vortex system and separated regions could be consequences of the combined effects of crossflow, embedded shock, and the compression fan reflected from the slip surface and impinging on the boundary layer.

Apart from the mutual interaction of boundary layers, the author also suggests that flow suction due to a pair of small vortices is another reason for sharp decrease of heating very near the corner centerline.

To achieve a better understanding of the corner flowfield, in particular inside the viscous layer, more investigations should be carried out.

Acknowledgments

This work was supported by the von Kármán Institute. The author wishes to acknowledge the encouragement given to him throughout this investigation by professors and technicians of the von Kármán Institute. Useful discussions with Onur Uzonur and Joe Stopper are gratefully acknowledged.

References

[1]Korkegi, R. H., "Survey of Viscous Interactions Associated with High Mach Number Flight," *AIAA Journal*, Vol. 9, No. 5, 1971, pp. 771–784.

[2]Stainback, P. C., "An Experimental Investigation at a Mach Number of 4.95 of Flow in the Vicinity of a 90° Interior Corner Aligned with the Free-Stream Velocity," NASA TN D-184, Feb. 1960.

[3]Stainback, P. C., "Heat Transfer Measurements at a Mach Number of 8 in the Vicinity of a 90° Interior Corner Aligned with the Free-Stream Velocity," NASA TN D-2417, Aug. 1964.

[4]Charwat, A. F., and Redekopp, L. G., "Supersonic Interference Flow Along the Corner of Intersecting Wedges," *AIAA Journal*, Vol. 5, No. 3, 1967, pp. 480–488.

[5]Watson, R. D., and Weinstein, L. M., "A Study of Hypersonic Corner Flow Interactions," *AIAA Journal*, Vol. 9, No. 7, 1971, pp. 1280–1286.

[6]Cresci, R. J., Rubin, S. G., Nardo, C. T., and Lin, T. C., "Hypersonic Interaction Along a Rectangular Corner," *AIAA Journal*, Vol. 7, No. 12, 1969, pp. 2241–2246.

[7]Cooper, J. R., and Hankey, W. L., "Flow Field Measurements in an Axisymmetric Axial Corner at $M = 12.5$," *AIAA Journal*, Vol. 12, No. 10, 1974, pp. 1353–1357.

[8]West, J. E., and Korkegi, R. H., "Supersonic Interaction in the Corner of Intersecting Wedges at High Reynolds Numbers," *AIAA Journal*, Vol. 10, No. 5, 1972, pp. 652–656; also Aerospace Research Lab., ARL 71-0241, Wright-Patterson AFB, OH, Oct. 1971.

[9]Korkegi, R. H., "On the Structure of Three-Dimensional Shock-Induced Separated Flow Regions," *AIAA Journal*, Vol. 14, No. 5, 1976, pp. 597–600.

[10]Hummel, D., "Axial Flow in Corners at Supersonic and Hypersonic Speeds," AGARD-R-764, Jan. 1990, pp. 5.1–5.37.

[11]Stainback, P. C., and Weinstein, L. M., "Aerodynamic Heating in the Vicinity of Corners at Hypersonic Speeds," NASA TN D-4130, Nov. 1967.

[12]Korkegi, R. H., "Effect of Transition on Three-Dimensional Shock-Wave/Boundary-Layer Interaction," *AIAA Journal*, Vol. 10, No. 3, 1972, pp. 361–363.

[13]Shang, J. S., Hankey, W. L., and Petty, J. S., "Three-Dimensional Supersonic Interacting Turbulent Flow Along a Corner," *AIAA Journal*, Vol. 17, No. 7, 1979, pp. 706–713.

[14]Papuccuoglu, H., "An Experimental Study of Hypersonic Axial Corner Flow," von Kármán Inst., VKI Project Rept. 1991-22, Brussels, Belgium, June 1991.

[15]Shang, J. S., and Hankey, W. L., "Numerical Solution of the Navier-Stokes Equations for a Three-Dimensional Corner," *AIAA Journal*, Vol. 15, No. 11, 1977, pp. 1575–1582.